CCNB1IP1 stabilizes MYCN through suppression of Fbxw7-mediated degradation and facilitates the growth of MYCN-amplified neuroblastoma

Bo Zhai (etyyzb@163.com)
Children's Hospital, Zhengzhou Children's Hospital
Yang Zhou
Hui Yan
Qiang Zhou
Penggao Wang
Fang Yang
Ziqiao Yuan
Yunjiang Zhou

Article

Keywords: MYCN amplification, Neuroblastoma, Cyclin B1 interacting protein 1, F box/WD-40 domain protein 7, Ubiquitination

Posted Date: July 28th, 2022

DOI: https://doi.org/10.21203/rs.3.rs-1876730/v1

Abstract

MYCN amplification is the most common genetic alteration and generally represents a negative prognosis for neuroblastoma (NB) patients. However, given the challenge of directly targeting MYCN, indirect strategies to modulate MYCN by interfering with its cofactors is attractive in NB treatment. Here, we showed that the cyclin B1 interacting protein 1 (CCNB1IP1) was highly expressed in MYCN-amplified (MYCN-AM) NB cell lines and patient-derived tumor tissues and closely associated with poor prognosis. Phenotypic studies confirmed that CCNB1I1P facilitated the proliferation and tumorigenicity of NB cells in cooperation with MYCN. Mechanistically, MYCN directly transactivated CCNB1IP1, which in turn attenuated the ubiquitination and degradation of MYCN protein, thus forming a positive feedback loop. Specifically, CCNB1IP1 competed with F box/WD-40 domain protein 7 (Fbxw7) for MYCN binding and enabled MYCN-mediated tumorigenesis in a C-terminal domain-dependent manner. Our research will provide new prospects for precise treatment of MYCN-AM NB based on MYCN-CCNB1IP1 interaction.

Introduction

NB is a sympathetic nervous system tumor originating from pluripotent migratory neural crest cells and is characterized with a higher mortality rate than other pediatric tumors (1, 2). Amplification of the MYCN gene is the most prevalent genetic alteration in NB patients and is one of the established adverse prognostic factors (3, 4). Currently, although multimodal treatment including surgery, myeloablative chemotherapy, radiotherapy and immunotherapy have benefited the low- and medium-risk patients, treatment outcomes for high-risk patients, especially those with MYCN amplification, remain suboptimal (5, 6). Therefore, elucidating the mechanism by which MYCN-driven malignant progression of NB and formulating the treatment strategy for high-risk NB with MYCN amplification has become a crucial issue in the field of NB treatment.

As a carcinogenic driver, MYCN participates in a variety of biological functions, such as tumor cell proliferation and metastasis, and works in the malignant progression of NB (3, 4). Unfortunately, as a consensus oncogene molecule, MYCN has neither a pocket structure that can be bound by small molecules nor enzyme activities that can be inhibited, rendering it almost impossible to be a direct target. At present, indirect strategies that interfere with the transcription, translation, protein stability and target gene transcription of MYCN offer a bright future for targeting MYCN-AM NB (7). Relevant targets developed based on these strategies have been presented, such as CDK7, AURKA, EZH2 (8–10). Nevertheless, there is still an urgent need to identify molecules with potential interactions and functional reciprocal support with MYCN as candidate targets for therapeutic applications.

Numerous studies have demonstrated that MYCN-AM and non-amplified (NA) NB cells exhibit significant differences in gene expression profiles (11). Indeed, certain target genes of MYCN that appear to be unnecessary for MYCN-NA NB cells have been reported to dominate the survival and malignant transformation of MYCN-AM NB cells. (9, 12). Based on this, we identified 22 shared differential genes (MYCN-AM vs. MYCN-NA, log2FC > 1, $P < 0.01$) including MYCN in 4 public datasets (TARGET, GSE49710,

GSE80149 and GSE120572). Among them, cyclin B1 interacting protein 1 (CCNB1IP1) appeared to be positively correlated with MYCN expression in NB samples and cell lines and was involved in poor long-term survival in NB patients. CCNB1IP1 was initially identified as an interacting protein of cyclin B1 involved in regulating cell cycle progression (13), and probably implicated in tumor events. Earlier, CCNB1IP1 was found as a component of HMG1C gene translocation fusion in uterine leiomyoma (14). Subsequently, overexpression of CCNB1IP1 mRNA was observed in metastatic melanoma and hepatocellular carcinoma (15, 16). However, there are some contradictory voices as well. In situ hybridization results confirmed the insufficient expression of CCNB1IP1 in colon cancer, breast cancer and non-small cell lung cancer (NSCLC) (15). Furthermore, CCNB1IP1 was indicated to have negative effect on cellular spreading, motility and invasion, but was required for cellular proliferation in gastric cancer cell U2OS and breast cancer cell MCF-7 (17). Nevertheless, it is worth noting that in the MYCN-driven NB mouse model of recurrent bone marrow metastasis CCNB1IP1 is significantly up-regulated (18). We hypothesized that CCNB1IP1 may contribute to MYCN-driven NB tumorigenesis and progression, however, the molecular basis of the effect of CCNB1IP1 on tumorigenicity, especially on MYCN-AM NB, remains elusive and warrants further investigation.

In present study, we found that CCNB1IP1 was overexpressed in MYCN-AM NB samples and cell lines, and was associated with the poor prognosis in NB patients. Silencing of CCNB1IP1 inhibited and its overexpression promoted the proliferation and growth of MYCN-AM NB cells in vitro and in vivo. Vitally, as a target gene of MYCN, CCNB1IP1 reciprocally stabilizes MYCN protein, forming a MYCN-CCNB1IP1 positive feedback regulatory loop. Degradation of MYCN is known to be mediated mainly through the F-box and WD-40 domain protein 7 (Fbxw7) E3 ligase pathway (19, 20). Mechanically, we found that CCNB1IP1 disrupted Fbxw7-dependent MYCN degradation through competing with Fbxw7 for MYCN binding and promoted oncogenicity in a C-terminal domain-dependent manner. Our study indicates that the MYCN-CCNB1IP1 interaction may be a promising therapeutic vulnerability for high-risk NB.

Results

CCNB1IP1 is overexpressed in MYCN-AM NB samples and cells and is associated with poor prognosis

In view of the “non-druggability” of MYCN, attempts to tackle MYCN have been focus on indirect targeting strategies. In addition to MYCN itself, some specific downstream genes of MYCN are specifically required for MYCN-AM NB growth (9, 12). To identify potential MYCN-dependent pro-survival genes, the publicly available transcriptome data from TARGET and GEO (GSE49710, GSE80149 and GSE120572) were obtained for analysis and comparison of differentially expressed genes between MYCN-AM and MYCN-NA NB samples or cell lines ($log_2FC>1$, $P<0.01$). As shown in Fig. 1A and Fig. S1A, a total of 22 shared differential genes, including MYCN, were identified from NB samples and cell lines. Correlation analysis revealed that CCNB1IP1 was positively correlated with MYCN expression in NB samples and cells in all datasets mentioned above (Fig. 1B and Fig. S1B-E). To extend this analysis to patient tumors, we

detected the expression of CCNB1IP1 in NB samples with or without MYCN amplification. As shown in Fig. 1C and D, CCNB1IP1 was overexpressed in NB patients with MYCN amplification compared to those with MYCN non-amplification. Specifically, high expression of CCNB1IP1(IHC score of moderate and strong) was observed in approximately 78.4% of MYCN-AM patients, whereas low expression of CCNB1IP1 (IHC score of low and negative) was detected in about 65.0% of MYCN-NA patients (Fig. 1E). Furthermore, CCNB1IP1 expression in NB patients was positively correlated with the amplification status (P<0.001, χ^2 test) and expression of MYCN, but not with gender (P = 0.240, χ^2 test) and age (P = 0.727, χ^2 test) (Fig. 1F). To better elucidate the relationship between CCNB1IP1 and MYCN amplification, protein levels of CCNB1IP1 and MYCN were detected by IB assay. It was found that CCNB1IP1 protein was significantly increased in MYCN-AM patients compared to those with NA and was positively correlated with MYCN expression (Fig. 1G and H). Similarly, the protein expression levels of CCNB1IP1 in NB cell lines were found to be significantly higher in MYCN-AM cell lines (SK-N-BE(2), BE(2)M17 and IMR32) compared to NA cell lines (SK-N-AS, SH-SY5Y and SK-N-SH) (Fig. 1I). These findings from NB samples and cells are substantially consistent with the bioinformatics analysis results from public datasets. Moreover, CCNB1IP1 expression was identified to be closely associated with NB patients prognostic (https://r2platform.com), with the higher expression of CCNB1IP1 associated with lower overall survival (OS) and disease progression-free survival (EFS) in NB patients (Fig. 1J-M). The above underscores the connection between CNB1IP11 overexpression and MYCN expression and the adverse prognosis of NB patients.

MYCN directly mediates the transcriptional activation of CCNB1IP1

Given the close correlation between the expression of CCNB1IP1 is closely related to the amplification or expression of MYCN, we speculate that there may exist mutual regulatory relationships between them. MYCN as a classical oncogenic transcription factor is involved in the positive regulation of several oncogenes, such as MDM2, MRP, E2F5 and ALDH18A1 (21–25), thus we considered whether the expression of CCNB1IP1 was regulated by MYCN. To verify this, the two constructed shRNA targeting MYCN with different sequences were transfected into MYCN-AM cell lines and their knockdown efficiency was examined. As shown in Fig. 2A, both MYCN-shRNA significantly interfered with the MYCN protein expression. As expected, ablation of MYCN significantly reduced both the CCNB1IP1 mRNA and protein in MYCN-AM NB cells (Fig. 2A and B). We noticed that the intracellular immunofluorescence (IF) intensity of CCNB1IP1 was obviously diminished upon MYCN knockdown as well (Fig. 2C). To fully confirm the regulation of MYCN on CCNB1IP1 expression, we exogenously overexpressed MYCN in a MYCN-NA cell lines and found a significant increase in mRNA and protein expression as well as IF staining intensity of CCNB1IP1 (Fig. 2D-F). To explore whether MYCN directly modulated the transcriptional activation of CCNB1IP1, we predicted the potential motifs of the CCNB1IP1 promoter region for MYCN binding (https://jaspar.genereg.net/). As shown in Fig. 2G, MYCN potentially interacts with the E-box of the CCNB1IP1 promoter region. For this, the reporter gene constructs contained CCNB1IP1 promoter with wild-type (WT) and E-box region mutant were established to confirm the transactivation of CCNB1IP1 by MYCN (Fig. 2H). As shown in Fig. 2I and J, the luciferase activity of the pGL3-CCNB1IP1 promoter was

significantly diminished or elevated in MYCN-AM cells and MYCN-NA cells upon silencing or overexpression of MYCN, respectively. Interestingly, the luciferase activity was significantly reduced upon E-box mutation and was unaffected even by the gain or loss of MYCN expression. Moreover, endogenous enrichment of MYCN to the E-box containing region was detected in the co-precipitated product of MYCN primary antibody by chromatin immunoprecipitation (CHIP) assay (Fig. 2K, L). The above results suggest that CCNB1IP1 is directly regulated at the transcriptional level as a downstream gene of MYCN.

CCNB1IP1 expression is essential for the proliferation and tumorigenic capacity of MYCN-AM NB cells

The high expression of CCNB1IP1 in MYCN-AM NB cells motivated us to wonder whether an excess of CCNB1IP1 facilitated MYCN-driven tumor-promoting function of NB cells. To verify this, we transfected CCNB1IP1-targeting shRNA into NB cells with different MYCN amplification status and examined cell growth and proliferation in vitro. As shown in the Fig. 3A and Fig. S2A, two shRNAs targeting CCNB1IP1 exhibited strong silencing efficiency in all six NB cell lines. As shown in Fig. 3B and Fig. S2B, CCNB1IP1 ablation resulted in a significant suppression of colony formation in MYCN-AM NB cells, while little effect was observed on MYCN-NA NB cells, except for a slight decrease in SK-N-SH transfected with shRNA#1. Besides, the growth of CCNB1IP1-deficient MYCN-AM NB cells, but not MYCN-NA NB cells, was significantly delayed upon CCNB1IP1 knockdown (Fig. 3C). To further clarify the effect of CCNB1IP1 on cell proliferation, EdU assay was also performed, and as shown in Fig. 3D and Fig. S2C, a significant reduction in the ratio of EdU-labeled NB cells was observed in CCNB1IP1-ablated MYCN-AM NB cells versus controls, but not in MYCN-NA NB cells. Meanwhile, enhanced cell proliferation was specifically observed in MYCN-AM NB cells upon CCNB1IP1 exogenously expressed, as manifested by an increase in the number of colony foci, accelerated cell growth, and an elevated proportion of EdU-labeled cells, whereas its effect on NA NB cells was inconsistent (Fig. 3E-H and Fig. S2D-G). To clarify the effect of CCNB1IP1 in NB tumorigenesis, CCNB1IP1-expressing or deficient NB cells-derived subcutaneous xenografts mouse model were constructed. Similar to the in vitro results, as shown in Fig. 3I-P, depletion of endogenous CCNB1IP1 impaired whereas exogenous overexpression of CCNB1IP1 facilitated the IMR32 cell-derived tumorigenesis. Altogether, these data suggest that CCNB1IP1 regulates the progression of NB appears to be largely dependent on the genetic amplification or expression of MYCN.

CCNB1IP1 stabilizes MYCN protein through suppressing its ubiquitin proteasome-dependent degradation.

It has been studied that some specific factors in the MYCN-driven gene expression profiling in turn influence the expression or stability of MYCN itself, thus forming a feedback regulatory circuit (25–27). The above findings confirmed that CCNB1IP1 was highly expressed as a MYCN target gene in MYCN-AM NB cells with a positive effect on their proliferation and tumorigenesis. To investigate whether CCNB1IP1 affects MYCN, we up- or down-regulated CCNB1IP1 in NB cells via transfection of overexpression plasmid or shRNA targeting CCNB1IP1, respectively. As shown in the Fig. 4A and B, the MYCN protein level was

significantly reduced in MYCN-AM NB cells with CCNB1IP1 knockdown, while the mRNA expression remained significantly unchanged. Similarly, we observed an upregulation of MYCN protein expression without altering mRNA expression in MYCN-expressing NA cells upon exogenous overexpression of CCNB1IP1 (Fig. 4C and D). Since MYCN expression at the transcriptional level was not affected by CCNB1IP1, we speculated whether it altered the post-translational stability of MYCN protein. For this, cycloheximide (CHX) chase assay was performed to evaluate the MYCN protein half-life. As shown in the Fig. 4E and F the degradation of MYCN protein was significantly accelerated upon CCNB1IP1 knockdown, while the half-life of MYCN protein was significantly prolonged with CCNB1IP1 overexpression. Treatment of NB cells with proteasome inhibitor MG132 resulted in increased MYCN protein levels that remained relatively high even under CCNB1IP1 knockdown, suggesting that CCNB1IP1 protects MYCN protein from ubiquitin proteasome-mediated degradation (Fig. 4G). We next performed (co-immunoprecipitation) co-IP assay and observed a dramatic increase in ubiquitination level of MYCN upon CCNB1IP1 knockdown in MYCN-AM NB cells (Fig. 4H). In reversal experiment, significant reduction in MYCN ubiquitination levels was detected in cells exogenously introduced with MYCN after overexpression of CCNB1IP1 (Fig. 4I). These data suggest that the function of CCNB1IP1 to stabilize MYCN protein is depend on its inhibition of proteasome-directed ubiquitination modifications.

The proliferation and tumorigenicity of NB mediated by CCNB1IP1 relies on MYCN expression

Since manipulation of CCNB1IP1 expression exhibited selective regulation of the proliferation and tumorigenic potential of MYCN-AM NB cells, we hypothesized that mRNA or protein expression of MYCN contribute to CCNB1IP1-mediated oncogenic effects. For this, CCNB1IP1 was overexpressed in NB cells with and without MYCN knockdown, and the cells growth and proliferation were examined by MTT and colony formation assays. As shown in Fig. 5A-C, the elevation of CCNB1IP1 by exogenous overexpression plasmid failed to alleviate the inhibition of cell growth and colony formation due to MYCN knockdown, indicating that maintenance of MYCN level is critical for CCNB1IP1 to foster cell growth and proliferation. To further clarify the effect of CCNB1IP1 on MYCN-AM NB cell tumor growth, we constructed Ctrl-, shMYCN- and shMYCN + CCNB1IP-IMR32 -derived subcutaneous xenograft tumor models. As shown in Fig. 5D-G, xenografts in the shMYCN group were significantly reduced in size, weight and growth rate compared with the Ctrl group, while tumor suppression was not alleviated in the shMYCN + CCNB1IP1 group even with rescue of CCNB1IP1 expression. In addition, IHC results confirmed that CCNB1IP1 immunostaining was attenuated in the MYCN knockdown group and rescued in the CCNB1IP1 overexpression group in tumor tissues (Fig. 5H). However, consistent with the tumor growth phenotype, restoration of CCNB1IP1 expression was not effectively reversed the tumor proliferation suppression caused by MYCN silencing (Fig. 5H). The above results suggest that the advantageous effect of CCNB1IP1 on NB cells proliferation and tumor growth depends on the high expression level of MYCN.

Stabilization of MYCN protein mediated by CCNB1IP1 is associated with disruption of Fbxw7-mediated ubiquitination

As a short-lived protein, MYCN stability tends to be tightly modulated by multiple intracellular proteasomal ubiquitin-dependent pathways involved in the several well-studied ubiquitin ligase or deubiquitinating enzyme, such as Trim32, Fbxw7, Huwe1, USP3 and USP5 (9, 28–31). Among them, Trim32, Fbxw7 and Huwe1 as ubiquitin ligase exert a negative regulatory effect in MYCN protein stability, while USP3 and USP5 as deubiquitinating enzyme elicited the opposite effect. Next, we wondered which signaling pathways were involved in CCNB1IP1-mediated stabilization of MYCN via post-transcriptional regulation. As shown in Fig. S3, ablation of CCNB1IP1 partially prevented the upregulation of MYCN protein level in Trim32 or Huwe1 knockdown cells, and overexpression of CCNB1IP1 differentially attenuated the downregulation of MYCN protein level caused by USP3 or USP5 silencing. However, no significant effect was observed in Fbxw7 knockdown cells (Fig. 6A). Surprisingly, exogenous co-expression of CCNB1IP1 greatly restored the Fbxw7-mediated down-regulation of MYCN (Fig. 6B). Besides, CCNB1IP1 expression did not obviously alter the protein expression level of Fbxw7 both in MYCN-AM and MYCN-NA NB cells. Compared to CCNB1IP1 knockdown alone, MYCN protein ubiquitination level was significantly decreased in IMR32 cell after Fbxw7 knockdown, but no further restorative elevation was observed after co-knockdown of CCNB1IP1 (Fig. 6C). In contrast, a significant inhibitory effect of elevated CCNB1IP1 expression on Fbxw7-mediated MYCN ubiquitination was observed in HEK293T cell exogenously expressed MYCN (Fig. 6D). This seems to indicate that the degradation of MYCN modulated by CCNB1IP1 may involve in its functional blockade of Fbxw7. To confirm whether the function of Fbxw7 is required for CCNB1IP1-regulated MYCN ubiquitination modification, we re-expressed Fbxw7 WT or function-deficient mutant F-box deletion mutant ($Fbxw7^{\triangle F-box}$) in Fbxw7-knockdown cells. As shown in Fig. 6E, overexpression of CCNB1IP1 significantly counteracted WT Fbxw7-induced MYCN ubiquitination, while it failed to cause further down-regulation of MYCN ubiquitination upon expression of Fbxw7 with an F-box deletion mutation. All these suggest that CCNB1IP1 stabilizes MYCN protein mainly as a result of blocking Fbxw7-dependent ubiquitination degradation of MYCN.

CCNB1IP1 maintains MYCN protein stability via competing with Fbxw7 for MYCN binding

It has been shown that the recognition and binding of MYCN by Fbxw7 determines the degradation of MYCN (19, 32). As shown in Fig. 7A, co-IP assay shown the endogenous interaction of CCNB1IP1 with MYCN in BE(2)M17 and IMR32 cells. Thus, we wondered whether CCNB1IP1 might affect the interaction of Fbxw7 with MYCN. As shown in Fig. 7B and Fig. S4, knockdown of CCNB1IP1 increased while overexpression of CCNB1IP1 blocked the binding of Fbxw7 to MYCN in a CCNB1IP1 expression-dependent manner. As described in Fig. 2C and F, endogenously or exogenously expressed MYCN and CCNB1IP1 were mostly co-localized in the nucleus of NB cells, which further corroborated their interaction. To further investigate the disruption of Fbxw7-MYCN interaction by CCNB1IP1, co-IP assay was performed in HEK293T cell transfected with the constructed plasmids encoding HA-MYCN and Flag-CCNB1IP1 WT or truncated mutants. As shown in Fig. 7C-D, HA-MYCN evidently interacted with Flag-CCNB1IP1 WT and M1-3 truncation mutants, but not with Flag-CCNB1IP1-M4 truncation mutant, suggesting that the C-terminal domain of CCNB1IP1 is a critical binding site for MYCN. It has been

previously shown that MYCN AA 48 to 89 determined the interaction with Fbxw7 (19). We next investigated the influence of MYCN AA 48 to 89 for the binding of MYCN between CCNB1IP1 and Fbxw7. As shown in Fig. 7E, Flag-CCNB1IP1 significantly restrained the co-binding of Myc-tagged Fbxw7 with HA-MYCN. However, the HA-MYCN mutant with deletion of AA 48 to 89 (HA-MYCN$^{\triangle 48-89}$) greatly impaired the capacity to bind both Myc-Fbxw7 and Flag-CCNB1IP1. And to fully characterize their interaction, the constructed expression vectors encoding the AA 48 to 89 of HA-MYCN (HA-MYCN$^{48-89}$), Flag-CCNB1IP1 WT, M4 and Myc-Fbxw7 were either separately or co-transfected into HEK293T cell. As shown in Fig. 7F, both Flag-CCNB1IP1 WT and Myc-Fbxw7 were able to interact with HA-tagged MYCN$^{48-89}$, whereas the Flag-CCNB1IP1 M4 mutant showed no physical binding to MYCN$^{48-89}$. In addition, Flag-CCNB1IP1 WT but not the M4 mutant was able to impair the Fbxw7-MYCN$^{48-89}$ interaction. Based on these results we also simulated the interaction between CCNB1IP1 and MYCN by computer-assisted protein-protein docking. As shown in Fig. 7G, the protein binding of CCNB1IP1 to MYCN was scored as -238.23 kcal/mol. The multiple interactions formed by residues in contact between CCNB1IP1 and MYCN proteins, such as hydrogen bonding and hydrophobic interactions, may effectively enhanced the stability of the protein complexes. Therefore, we conclude that CCNB1IP1 is able to bind the identical MYCN amino acid region to Fbxw7, and also reveal that the competitive binding effect of CCNB1IP1 is responsible for the escape of MYCN from Fbxw7-mediated ubiquitination degradation.

CCNB1IP1 stabilizes MYCN and promote oncogenicity in a C-terminal domain-dependent manner

Above results suggested that the C-terminal domain of CCNB1IP1 is essential for competitive binding of MYCN with Fbxw7. To further clarify whether this region is required for MYCN stability, we knockdown CCNB1IP1 in IMR32 cell and re-expressed CCNB1IP1 WT or M4 mutant and the MYCN protein degradation detected was detected by CHX-chase assay. As shown in Fig. 8A and B, overexpression of CCNB1IP1 WT but not M4 mutant significantly rescued the reduction in MYCN half-life caused by CCNB1IP1 knockdown. Interestingly, overexpression of CCNB1IP1 WT was able to, whereas the M4 mutant of CCNB1IP1 was unable to suppress the ubiquitination of MYCN and stabilize its protein level (Fig. 8C). To verify whether this stabilizing effect of CCNB1IP1 is associated with its interference with Fbxw7, we re-expressed CCNB1IP1 WT and M4 mutant in CCNB1IP1 knockdown NB cells with or without Fbxw7 silencing. As shown in Fig. 8D, silencing Fbxw7 significantly upregulated MYCN protein level in cells knockdown of CCNB1IP1, while there was no obvious effect on the restoration of MYCN protein in cells re-expressing CCNB1IP1 WT. However, re-expressing M4 mutant failed to reverse the down-regulation of MYCN protein and to further interfere with the regulation of MYCN expression by Fbxw7. Given that CCNB1IP1 regulated the protein stability of MYCN and is involved in MYCN-AM NB cells proliferation and oncogenesis, we speculated whether the function of CCNB1IP1 in stabilizing MYCN protein determines its oncogenicity. As shown in Fig. 8E, the colony-forming ability of MYCN-AM NB cells re-expressed M4 mutant was significantly diminished compared to those transfected with CCNB1IP1 WT. To this end, in vivo experiments were also conducted with an IMR32 cell-derived xenografts mouse model. As shown in Fig. 8F-I, IMR32-shCCNB1IP1 cell re-expressing CCNB1IP1 M4 mutant showed significant tumor growth

inhibition compared to cells re-expressing CCNB1IP1 WT. The data suggest that C-terminal domain of CCNB1IP1-mediated deubiquitination and stabilization of MYCN are essential for tumorigenesis in NB.

Discussion

MYCN amplification is a key bottleneck restricting the overall efficacy of NB and is one of the major causes of treatment failure. Disrupting MYCN expression impedes proliferation and metastasis and induces differentiation and death of MYCN-AM NB cells (33–35). Although MYCN deserves to be considered as an attractive candidate target for high-risk NB, direct targeting of MYCN proteins is fraught with challenges owing to the lack of surface structures for small molecules binding and the enzymatic activity that can be specifically inhibited. Given this, indirect targeting strategies through manipulating interactive molecules associated with MYCN have been rapidly discovered and developed over the years, which has become a research hotspot in the NB field. The alternative MYCN-targeting strategies mainly involve the transcription, translation, protein stability and target gene transcription of MYCN (7). For example, ALDH18A1 has been reported as a target gene of MYCN and its protein reciprocally participates in the regulation of MYCN transcriptional activation, thus forming a positive feedback loop (25). YG1702 was identified as an inhibitor of ALDH18A1 based on a computer-assisted virtual screen and displayed potent inhibition of MYCN-driven tumorigenicity in cellular and animal experiments. Aurora-A was reported to bind to MYCN protein through the same motif recognized by Fbxw7 ubiquitin ligase in MYCN Box I domain, resulting in an effective reduction of MYCN affinity for Fbxw7 (9, 19). Currently, MLN8237 (alisertib) has been investigated in clinical trials for the treatment of recurrent NB as an inhibitor capable of distorting the Aurora-A conformation (36, 37). Similarly, the polycomb repressive complex 2 component EZH2 was shown to counteract Fbxw7-mediated polyubiquitination and proteasomal degradation of MYCN by competing with Fbxw7 for MYCN binding in a methyltransferase-independent manner (38). And the EZH2 depleting agent DZNep but not the enzyme inhibitor was found to induce the degradation of MYCN and arrest the growth of tumor cells (38). Moreover, EZH2 is directly positively regulated by MYCN transcriptionally and is also involved in MYCN-mediated transcription of some target genes (10, 38, 39). These indicate that drug development based on the identified key molecules that regulate MYCN or are regulated by MYCN will definitely be a promising approach.

Studies have confirmed that there are significant differences in gene expression profiles between MYCN-AM and NA NB. In addition to MYCN itself, the growth of MYCN-AM NB cells is highly dependent on the certain genes downstream of MYCN, that are unnecessary for MYCN-NA NB cells (9, 12). Encouragingly, manipulation of these genes would selectively suppress the malignant biological phenotype of MYCN-AM NB, which exemplifies the promising potential of this strategy in drug development and clinical applications (32, 40, 41). Therefore, it is of profound relevance to search for potential regulatory factors and elaborate new strategies based on the specific activation pathways of MYCN amplification from the perspective of "selective inhibition". Here, we identified 22 shared differential genes based on transcriptomic differences between MYCN-AM and NA NB tissues and cells in multiple datasets (Fig. 1A-B), which also contain several potential targets for NB that have been and are being investigated in NB, such as ODC1, PHGDH and AURKB (42–44). Gene expression correlation analysis revealed a high

positive correlation between CCNB1IP1 and MYCN expression in all the four datasets (Fig. 1C-G). Our results showed that CCNB1IP1 was overexpressed in both MYCN-AM NB patient specimens and cell lines, which is consistent with the database analysis (Fig. 2A-G). And its higher expression level is closely associated with lower OS, EFS of patients, which further implied the malignant function of CCNB1IP1 in NB. All these have aroused our curiosity about the role and function of CCNB1IP1 in MYCN-AM NB (Fig. 2H-K).

CCNB1IP1 was initially identified as an interacting protein of cyclin B1 for the regulation of cell cycle progression (13). To date, the biological function of CCNB1IP1 in a variety of tumors has been noted in several studies. Some of these studies stand on the side that CCNB1IP1 may produce a positive effect on tumorigenesis. Earlier, CCNB1IP1 was found to be a component of HMG1C gene translocation fusion in uterine leiomyoma, but its biological effect has hardly been discussed (14). Similarly, CCNB1IP1 was found aberrantly overexpressed in metastatic melanoma and hepatocellular carcinoma (15, 16). However, some results contradicting the above studies have also been reported. In an in-situ hybridization study based on patient-derived tumor tissue microarrays from multiple cancer types, CCNB1IP1 was observed to be under-expressed in colorectal, breast and non-small cell lung cancer (NSCLC), and its expression level was negatively correlated with survival time in adenocarcinoma, small cell squamous carcinoma and NSCLC (15). Furthermore, silencing of CCNB1IP1 in gastric cancer cells U2OS and breast cancer cells MCF-7 promoted cells metastasis and invasion, but suppressed cells proliferation and growth, suggesting that the extent or nature of CCNB1IP1 being required in different biological behaviors of tumor cells may not be consistent (17). Notably, a recent study based on transcriptome analysis of a MYCN-driven NB mouse model revealed that CCNB1IP1 was highly expressed in recurrent metastatic tissues (18). Although the role of CCNB1IP1 has not been further investigated, the results partially implicated an oncogenic function of CCNB1IP1 in NB. In this study, a significant oncogenic driving effect of CCNB1IP1 on MYCN-expressing or AM NB cells was found in cellular and xenograft tumor studies, as manifested by a greater proliferation and tumor formation, while having little effect on cells with low MYCN expression or NA. In contrast, even restoration of CCNB1IP1 expression failed to rescue the diminished proliferative capacity and tumor growth of NB cells caused by MYCN deficiency (Fig. 6). We hypothesized that the oncogenic effect of CCNB1IP1 probably exerts effectively in NB cells with abnormally high expression of MYCN, whereas in MYCN-NA cells, a gene network sufficient for CCNB1IP1-induced cell carcinogenesis seems to be infeasible. All these inspired us that CCNB1IP1 may cooperate with MYCN to drive the tumorigenic development of NB, and its specific biological role in NB needs to be further explored in a mouse model of NB primary that better resembles the characteristics of tumorigenesis and progression.

Interestingly, CCNB1IP1 acts as the target gene of MYCN that reciprocally maintained the protein stability of MYCN (Fig. 5). Interfering with the post-transcriptional stability or activity of MYCN is relatively straightforward and is receiving increasing attention to develop more effective and feasible options to attack MYCN. According to our data, the regulation of MYCN protein ability by CCNB1IP1 is mainly associated with E3 ubiquitin ligase Fbxw7 and is not dependent on other partner molecules interacting with MYCN (Trim32, Huwe1, USP3 and USP5) (Fig. 7 and Fig. S2) (9, 28–31). In truncated mutation experiments, we found that CCNB1IP1 bound tightly to the reciprocal region of Fbxw7 on MYCN AA 48–

89 in a C-terminal domain-dependent manner (Fig. 8). Interestingly, MYCN with deletion mutations in this region lost its ability to bind Fbxw7, and binding to CCNB1IP1 was also significantly abolished (Fig. 8). This indicates that the Fbxw7 binding segment is contained at least within the region where MYCN interacts with CCNB1IP1. In contrast, the MYCN AA 48–89 region is not be required for the binding of other MYCN cofactors (Trim32, Huwe1, USP3 and USP5). Therefore, CCNB1IP1 would not disturb their binding to MYCN or further affect the stability of MYCN protein, which presumably corroborated with the results in Fig. 7 and Fig. S2.

Currently, numerous studies suggest that destabilization of MYCN has great potential as an emerging therapeutic strategy, although it also faces various obstacles, such as specificity and clinical translation issues. For example, AURKA kinase is currently being studied as a well-established therapeutic target for MYCN-AM NB. Based on the interaction of AURKA with MYCN, several small molecules have been identified which can bind to AURKA and alter its conformation to disrupt the Fbxw7-MYCN complex and cause rapid MYCN degradation (9, 45). Among them, inhibitor alisertib was assumed to be effective in uncoupling the direct interaction of the catalytic domain of AURKA with MYCN and displayed good activity against pediatric solid tumors in preclinical trials (46). Moreover, the inhibitory effect of AURKA on tumors is not absolutely dependent on the state of MYCN amplification, as evidenced by the fact that a few Myc-driven tumors are also sensitive to AURKA suppression (47, 48). Whereas in clinical trials including NB, inhibition of AURKA resulted in significant unintended toxicity and largely disappointing responses (36, 37). Encouragingly, good responses were achieved in phase I and II clinical trials of alisertib in combination with irinotecan and temozolomide for the treatment of relapsed or refractory neuroblastoma, conferring a potentially more favorable application of this inhibitor in combination with chemotherapeutic drug therapies (49, 50). As targets for MYCN-AM NB are still limited or unspecific, the discovery and development of new targets and therapeutic applications remains urgent. Here, our results and those of others adequately indicate that destabilization of MYCN is going to be an overwhelming breakthrough in attacking MYCN NA NB. we demonstrated that CCNB1IP1 supported MYCN-AM NB cells proliferation and tumor growth by repressing Fbxw7-mediated ubiquitination degradation of MYCN through gain- and loss-of-function experiments. Moreover, CCNB1IP1 antagonized the interaction of Fbxw7 with MYCN in a competitive binding manner, during which the C-terminal domain of CCNB1IP1 is required (Fig. 10).

Here, we identified CCNB1IP1 as a novel cofactor that stabilizes MYCN and acts synergistically with MYCN to enhance the proliferation and tumorigenicity of NB cells. Mechanistically, CCNB1IP1 blocked MYCN degradation through competitive binding of MYCN to Fbxw7, which further diversified the regulatory mechanism of MYCN proteostasis. Our data supported the potential of CCNB1IP1 as a MYCN-specific intervention target. However, there remain certain limitations and pending issues to be addressed in our study. Although phenotypic effects were observed, further investigation may be required to clarify how the synergistic effect of CCNB1IP1 with MYCN modulates the tumorigenicity of NB cells. Given the cell cycle-dependent expression and nucleus co-localization of both CCNB1IP1 and MYCN, it is necessary to further explore the complexity and spatiotemporal-dependent alterations of their interactions. Therefore, multifaceted mechanistic studies need to be integrated to more accurately assess the extent to

which CCNB1IP1 contributes to the post-transcriptional regulation of MYCN expression. Although no definitive inhibitor of CCNB1IP1 has been developed, our study indicates that targeting CCNB1IP1 may be a new option for the future treatment of MYCN-AM NB. Screening and validation of small molecule compounds or agents with known clinical indications that specifically disrupt the interaction of CCNB1IP1 with MYCN as candidate inhibitors would be expected to be available for preclinical testing and subsequent clinical applications of MYCN AM NB. Although targeting CCNB1IP1 is still far from clinical application, it remains undeniable that NB cell growth is impaired by disrupting the CCNB1IP1-MYCN interaction. Ideally, more effective drug combination regimens could be developed based on this idea to provide more effective and specific treatments for improving prognosis and survival of high-risk NB patients.

Material Methods

Cell lines and culture

Human NB cell lines SK-N-BE (2), SK-N-SH and SH-SY5Y and HEK293T were obtained from Cell Bank of the Chinese Academic of Sciences (Shanghai, China), SK-N-AS, IMR32 and BE(2)M17 were purchased from FuHeng biology (Shanghai, China). SK-N-SH and IMR32 were cultured in MEM medium with 10% FBS. SK-N-BE (2), SH-SY5Y and BE(2)M17 were cultured in DMEM/F-12 medium with 10% FBS. SK-N-AS and HEK293T were cultured in DMEM medium with 10% FBS. All cell lines were authenticated by short tandem repeat profiling analysis performed at Biowing Applied Biotechnology Co., Ltd. (Shanghai, China). and maintained according to the manufacturer's instructions and cultured in a humidified incubator containing 5% CO2 at 37°C.

Reagents and antibodies

MTT (purity ≥ 98%) was purchased from Sigma-Aldrich (St. Louis, USA, 88417). Cycloheximide (CHX, purity ≥ 99.81%) was purchased from MedChemExpress (NJ, USA, HY-12320). MG132 was purchased from Selleck Chemicals Inc (Houston, USA, S2619). AceQ qPCR SYBR Green Master Mix was purchased from Vazyme (Nanjing, China). First-strand cDNA Synthesis super Mix kit, RIPA buffer and TRIzol reagent were obtained from Sparkjade Biotech (Shandong, China). Endotoxin-free plasmid small extraction medium extraction kit was purchased from Tiangen. Immunohistochemistry (IHC) kits were purchased from Vector Laboratories. Dual Luciferase Reporter Gene Assay Kit, CHIP kit, EdU adulteration assay kit and Lipo8000 transfection reagent were purchased from Beyotime Biotech (Hangzhou, China). Fetal bovine serum was purchased from Sigma-Aldrich (St. Louis, MO, United States). Serum-free lyophilization solution, rapid blocking solution, and universal antibody dilutions were purchased from New Cell & Molecular Biotech. IP/CoIP Kit (Magnetic Beads) was purchased from Dia-An Biotech, Inc (Wuhan, China). Primary antibodies we used as follows: anti-Flag, anti-HA, anti-His and anti-Myc and anti-β-actin were purchased from Abways Technology, anti-CCNB1IP1 was purchased from Huabio, anti-MYCN was purchased from Cell Signaling Technology, anti-Fbxw7 was purchased from Abcam (Cambridge, MA,

United States), anti-USP3, anti-USP5, anti-Trim32 and anti-Ubiqiutin were purchased from Proteintech Group. Fluorescent secondary antibodies were purchased from Keygen Biotech (Shanghai, China).

RNA isolation, qRT-PCR

Total RNA was extracted, reverse transcribed and subjected to PCR as previously described (51). Primer sequences for qRT-PCR analysis are listed in Supplementary Table S1. β-actin expression was used for normalization. Relative expression of target genes was normalized using the internal control β-actin and calculated using the $2^{-\Delta\Delta Cq}$ method.

Protein preparation and IB assay

NB cells or patient-derived tissues placed on ice were lysed with RIPA lysate containing 1 mM PMSF. Protein concentrations in the obtained lysates were assessed using the BCA method. The denatured proteins were separated by SDS-PAGE and transferred to polyvinylidene fluoride membranes (Millipore, USA). After closure with Rapid Closure Solution, incubate overnight at 4°C using the appropriate primary antibody. Following washing with PBST, incubate for 1–2 hours at 37 ℃ using the appropriate secondary antibody and wash again with PBST. Protein signals were visualized under a Bio-Rad gel imaging system using ECL chromogenic reagents. β-actin was used as a loading control.

Co-IP assay

Co-IP assay was performed using the IP/CoIP Kit (Magnetic Beads) according to the manufacturer's instructions. Briefly, cell lysates were preparation and collected. Incubation of antibodies with magnetic beads. Binding of the antigen to antibody-magnetic bead complex. Separated the magnetic beads, added the appropriate amount of loading buffer and boiled at 95°C for 5min, for sample elution. The eluted samples were subjected to SDS-PAGE and IB assay to detect specific proteins.

Protein half-life detection

The stability of MYCN protein was examined in cells with specific knockdown or overexpression. CHX-chase analysis was performed to determine the protein half-life of MYCN. CHX treatment inhibited the intracellular protein synthesis process thereby facilitating accurate detection of protein degradation. Briefly, in the MYCN half-life assay, the target cells were incubated with CHX (10 μg/ml) for the indicated time, and then the cells were harvested and relative protein expression of MYCN was measured by IB analysis.

Dual-luciferase reporter assay

CCNB1IP1 promoter sequence wild-type and mutant constructs were transfected with the internal control vector Renilla into specifically treated NB cells according to the manufacturer's instructions. Then the luciferase assays were performed using the Dual Luciferase Reporter Gene Assay Kit (Beyotime Biotech, Hangzhou, China) as previously described (52). The luciferase activity was normalized to Renilla expression for each sample.

CHIP

CHIP was performed according to manufacturer's instructions. Briefly, cells transfected with specific silencing or overexpression plasmids were collected, cross-linked and sonicated. IP assay was performed with anti-MYCN antibody co-incubated with the lysis products. IgG was used as a loading control. Immunoprecipitation complexes were obtained and purified, and the binding of MYCN to the CCNB1IP1 promoter was detected by semi-quantitative PCR. The primers used to amplify the putative binding CCNB1IP1 promoter fragment were listed in Supplementary Table S2.

Colony formation assay

The procedure was performed as previously described (52). NB cells stably expressing or silencing specific genes were seeded into six-well plates at an amount of 500 per well and cultured for approximately two weeks. At the end of the culture, the medium was discarded, washed three times with cold sterile 1×PBS, fixed in 4% formaldehyde and stained with 0.1% crystal violet. The colonies number was then counted macroscopically.

EdU incorporation assay

EdU incorporation assay was performed according to manufacturer's instructions. Briefly, the target cells transfected with CCNB1IP1 overexpression plasmids or shRNA were seeded into 96 well plates at an amount of 5000 per well. Cells were fixed with 4% neutral paraformaldehyde and permeabilized with 0.5% Triton X-100 following incubation with EdU. Then the click EdU reactions were performed and the cells were placed under an inverted fluorescent microscope for observation and photography.

Ubiquitination analysis

Target cells were transfected with plasmids expressing or silencing specific proteins, and then protein lysates were collected and prepared. IP assay was performed with anti-MYCN or anti-HA-MYCN antibodies. The MYCN protein polyubiquitination in the co-IP products was subsequently determined by IB assay with anti-ubiquitin primary antibody. The IgG group was set as a loading control.

Cell transfection

The shRNA targeting CCNB1IP1 (#1 TRCN0000003418 and #2 TRCN0000003419) and MYCN (#1 TRCN0000020695 and #2 TRCN0000020698) in pLKO.1 lentiviral vector were purchased from Millipore Sigma (St. Louis, MO) and used as recommended by the manufacturer. The packaging plasmids PsPAX2 and pMD2.G were purchased from the MiaoLing Plasmid Sharing Platform. Targeting sequences of shRNA for Fbxw7, Trim32, Huwe1, USP3 or USP5 are listed in Supplementary Table S3. The Flag-tagged coding sequence of CCNB1IP1 WT or the relevant M1-M4 mutants, HA-tagged MYCN WT or the relevant $MYCN^{48-89}$ and $MYCN^{\triangle 48-89}$ mutants, Myc-tagged Fbxw7 WT and or the $Fbxw7^{\triangle F-box}$ mutant were cloned into the lentiviral vector, pCDH-CMV-MCS-EF1-GFP + Puro (Changsha Youze Biotechnology Co., Ltd) to generate expression plasmids. The relevant lentiviral particles were generated in HEK293T cell using the Lentiviral Packaging Kit according to the manufacturer's instructions. As for cell transfection,

the target cells were transfected with lentiviral-encoded target DNA constructs using lipo8000 transfection reagent according to the manufacturer's instruction and stable transfected cells were selected with puromycin (1μg/ml).

Protein-protein docking

Preparation of protein structure: CCNB1IP1, MYCN target protein structures were predicted by I-TASSER online server (https://zhanggroup.org//I-TASSER/). All protein structures were treated in a molecular manipulation environment (MOE 2019.1) including removal of water and ions, protonation, addition of missing atoms and complement of missing groups, and protein energy minimization. Molecular docking: The processed CCNB1IP1 and MYCN proteins were introduced into the receptor and ligand modules of HDOCK software respectively, and the docking sites were selected to be the whole surface of the protein, and the conformation of protein-protein complex was set to 100, a hybrid algorithm for template-based and template-free Docking automatically predicted its interaction and was evaluated using a Docking Score as well as the RMSD of the ligand, visualizing the Docking results with selected Pymol2.1 software.

Animal procedures

Balb/c male nude mice purchased from Vitone River Laboratory Animal Technology Co., Ltd. were housed in a standard SPF animal room equipped with sealed air filtration devices. All experimental procedures on mice were approved by the Animal Ethics Committee of Zhengzhou University and performed in accordance with the institutional guidelines. The mice were randomly grouped and subjected to a period of acclimatization prior to the experiment. Mice were injected with IMR32 cell (200 μl, 2×10^6 cells) stably transfected with non-targeted shRNA (shCtrl), CCNB1IP1-targeted shRNA (shCCNB1IP1#1 and #2); empty vector (Vector) or CCNB1IP1 overexpression plasmid; MYCN-targeted shRNA (shMYCN) or MYCN-targeted shRNA combined with CCNB1IP1 plasmid (shMYCN + CCNB1IP1) in the subcutaneous space to construct NB cells-derived xenograft tumor models. For tumor growth assay, subcutaneous tumor volumes were measured every 5 days, and mice were euthanized at the end of the experiment, then tumors were peeled and weighed. The volume was calculated by the formula: $V= (a \times b^2)/2$, where **a** and **b** are the long axis and short axis of tumor, respectively.

IHC detection

IMR32-derived xenogeneic tissues from nude mice or primary tumor tissues from untreated NB patients were obtained and fixed in 4% paraformaldehyde, dehydrated in an alcohol gradient, hyalinized in xylene, paraffin embedded. IHC staining for CCNB1IP1, MYCN and ki67 expression was performed using the appropriate primary antibodies following the manufacturer's instructions of IHC kit. All sections were photographed under a vertical microscope (Nikon, Japan). The sections were analyzed with a double-blind method employing a semi-quantitative scoring system as previously reported (53).

Histological Sample

This study was approved by the ethics review committee of Zhengzhou University according to the standards and guidelines of the institutional review committee (No. 2021-H-K24). All samples involved in

this study were untreated primary tumors from NB patients with defined MYCN amplification status. And patients were signed written informed consent in the Children's Hospital Affiliated to Zhengzhou University upon admission. All studies on human samples were conducted in accordance with accepted ethical norms (Helsinki declaration, CIOMS, Belmont Report, American common rules).

Dataset analysis

RNA sequencing data for NB patients and cell lines and clinical follow-up information for patients were download from the Gene Expression Omnibus (GEO) database (https://www.ncbi.nlm.nih.gov/geo/, GEO accession numbers: GSE49710, GSE120572, GSE80149) and the Therapeutically Applicable Research to Generate Effective Treatments (TARGET) data portal (https://ocg.cancer.gov/programs/target). A total of 145, 493 and 393 patients and 5 NB cell lines containing complete gene expression data and a defined MYCN amplification status (AM or NA) were included in this study following filtering out some samples with incomplete information. For the analysis of overall survival and disease-free progression survival, patients were divided into a CCNB1IP1 high expression group (top 25%) and a CCNB1IP1 low expression group (bottom 75%), and Kaplan-Meier curves were created using an online genomic analysis visualization platform (https://r2platform.com).

Statistical Analysis

Data obtained from at least three independent experiments were expressed as mean ± SD. Statistical analysis was performed using SPSS version 25.0. Student's t-test and one-way ANOVA was calculated to compare the differences between two groups or multiple groups, respectively. Statistically significant difference was shown as $^{*}P < 0.05$, $^{**}P < 0.01$, and $^{***}P < 0.001$.

Declarations

Acknowledgments

This work was supported by grants from the Henan medical science and technology project (LHGJ20210629, LHGJ20190958, LHGJ20190889), and the Scientific and Technological Projects of Henan province (222102310026), and the research startup funding (Children's Hospital Affiliated to Zhengzhou University). We gratefully acknowledge the experimental equipment platform and financial support granted by Children's Hospital Affiliated to Zhengzhou University.

Declaration of competing interest

The authors declare that they have no known competing financial interests or personal relationships that could have appeared to influence the work reported in this paper.

Authors' contributions

Bo Zhai and Yang Zhou: Conceptualization, Funding acquisition, Supervision, Methodology. Yang Zhou, Hui Yan and Yunjiang Zhou: Investigation, Data curation, Writing- Original draft preparation, Software.

Penggao Wang and Fang Yang: Visualization, Software, Validation. Qiang Zhou: Resources. Ziqiao Yuan: Writing- Reviewing and Editing.

References

1. Qiu B, Matthay KK. Advancing therapy for neuroblastoma. Nature Reviews Clinical Oncology. 2022.
2. Maris JM, Hogarty MD, Bagatell R, Cohn SL. Neuroblastoma. Lancet (London, England). 2007;369(9579):2106–20.
3. Otte J, Dyberg C, Pepich A, Johnsen JI. MYCN Function in Neuroblastoma Development. 2021;10.
4. Huang M, Weiss WA. Neuroblastoma and MYCN. Cold Spring Harbor perspectives in medicine. 2013;3(10):a014415.
5. Bosse KR, Maris JM. Advances in the translational genomics of neuroblastoma: From improving risk stratification and revealing novel biology to identifying actionable genomic alterations. Cancer. 2016;122(1):20–33.
6. Ryan AL, Akinkuotu A, Pierro A, Morgenstern DA, Irwin MS. The Role of Surgery in High-risk Neuroblastoma. Journal of pediatric hematology/oncology. 2020;42(1):1–7.
7. Rickman DS, Schulte JH, Eilers M. The Expanding World of N-MYC-Driven Tumors. Cancer discovery. 2018;8(2):150–63.
8. Chipumuro E, Marco E, Christensen CL, Kwiatkowski N, Zhang T, Hatheway CM, et al. CDK7 inhibition suppresses super-enhancer-linked oncogenic transcription in MYCN-driven cancer. Cell. 2014;159(5):1126–39.
9. Otto T, Horn S, Brockmann M, Eilers U, Schüttrumpf L, Popov N, et al. Stabilization of N-Myc is a critical function of Aurora A in human neuroblastoma. Cancer cell. 2009;15(1):67–78.
10. Dardenne E, Beltran H, Benelli M, Gayvert K, Berger A, Puca L, et al. N-Myc Induces an EZH2-Mediated Transcriptional Program Driving Neuroendocrine Prostate Cancer. Cancer cell. 2016;30(4):563–77.
11. Berwanger B, Hartmann O, Bergmann E, Bernard S, Nielsen D, Krause M, et al. Loss of a FYN-regulated differentiation and growth arrest pathway in advanced stage neuroblastoma. Cancer cell. 2002;2(5):377–86.
12. Valsesia-Wittmann S, Magdeleine M, Dupasquier S, Garin E, Jallas AC, Combaret V, et al. Oncogenic cooperation between H-Twist and N-Myc overrides failsafe programs in cancer cells. Cancer cell. 2004;6(6):625–30.
13. Toby GG, Gherraby W, Coleman TR, Golemis EA. A novel RING finger protein, human enhancer of invasion 10, alters mitotic progression through regulation of cyclin B levels. Molecular and cellular biology. 2003;23(6):2109–22.
14. Mine N, Kurose K, Konishi H, Araki T, Nagai H, Emi M. Fusion of a sequence from HEI10 (14q11) to the HMGIC gene at 12q15 in a uterine leiomyoma. Japanese journal of cancer research: Gann. 2001;92(2):135–9.

15. Confalonieri S, Quarto M, Goisis G, Nuciforo P, Donzelli M, Jodice G, et al. Alterations of ubiquitin ligases in human cancer and their association with the natural history of the tumor. Oncogene. 2009;28(33):2959–68.
16. Fang X, Yang D, Luo H, Wu S, Dong W, Xiao J, et al. SNORD126 promotes HCC and CRC cell growth by activating the PI3K-AKT pathway through FGFR2. Journal of molecular cell biology. 2017;9(3):243–55.
17. Singh MK, Nicolas E, Gherraby W, Dadke D, Lessin S, Golemis EA. HEI10 negatively regulates cell invasion by inhibiting cyclin B/Cdk1 and other promotility proteins. Oncogene. 2007;26(33):4825–32.
18. Yogev O, Almeida GS, Barker KT, George SL, Kwok C, Campbell J, et al. In Vivo Modeling of Chemoresistant Neuroblastoma Provides New Insights into Chemorefractory Disease and Metastasis. Cancer research. 2019;79(20):5382–93.
19. Richards MW, Burgess SG, Poon E, Carstensen A, Eilers M, Chesler L, et al. Structural basis of N-Myc binding by Aurora-A and its destabilization by kinase inhibitors. Proceedings of the National Academy of Sciences of the United States of America. 2016;113(48):13726–31.
20. Welcker M, Orian A, Jin J, Grim JE, Harper JW, Eisenman RN, et al. The Fbw7 tumor suppressor regulates glycogen synthase kinase 3 phosphorylation-dependent c-Myc protein degradation. Proceedings of the National Academy of Sciences of the United States of America. 2004;101(24):9085–90.
21. Slack A, Lozano G, Shohet JM. MDM2 as MYCN transcriptional target: implications for neuroblastoma pathogenesis. Cancer letters. 2005;228(1–2):21–7.
22. Manohar CF, Bray JA, Salwen HR, Madafiglio J, Cheng A, Flemming C, et al. MYCN-mediated regulation of the MRP1 promoter in human neuroblastoma. Oncogene. 2004;23(3):753–62.
23. Liu Y, Liu D, Wan W. MYCN-induced E2F5 promotes neuroblastoma cell proliferation through regulating cell cycle progression. Biochemical and biophysical research communications. 2019;511(1):35–40.
24. Norris MD, Bordow SB, Haber PS, Marshall GM, Kavallaris M, Madafiglio J, et al. Evidence that the MYCN oncogene regulates MRP gene expression in neuroblastoma. European journal of cancer (Oxford, England: 1990). 1997;33(12):1911-6.
25. Guo YF, Duan JJ, Wang J, Li L, Wang D, Liu XZ, et al. Inhibition of the ALDH18A1-MYCN positive feedback loop attenuates MYCN-amplified neuroblastoma growth. Science translational medicine. 2020;12(531).
26. Koach J, Holien JK, Massudi H, Carter DR, Ciampa OC, Herath M, et al. Drugging MYCN Oncogenic Signaling through the MYCN-PA2G4 Binding Interface. Cancer research. 2019;79(21):5652–67.
27. Marshall GM, Liu PY, Gherardi S, Scarlett CJ, Bedalov A, Xu N, et al. SIRT1 promotes N-Myc oncogenesis through a positive feedback loop involving the effects of MKP3 and ERK on N-Myc protein stability. PLoS genetics. 2011;7(6):e1002135.

28. Izumi H, Kaneko Y. Trim32 facilitates degradation of MYCN on spindle poles and induces asymmetric cell division in human neuroblastoma cells. Cancer research. 2014;74(19):5620–30.
29. Zhao X, Heng JI, Guardavaccaro D, Jiang R, Pagano M, Guillemot F, et al. The HECT-domain ubiquitin ligase Huwe1 controls neural differentiation and proliferation by destabilizing the N-Myc oncoprotein. Nature cell biology. 2008;10(6):643–53.
30. Nagy Z, Seneviratne JA, Kanikevich M, Chang W, Mayoh C, Venkat P, et al. An ALYREF-MYCN coactivator complex drives neuroblastoma tumorigenesis through effects on USP3 and MYCN stability. Nature communications. 2021;12(1):1881.
31. Cheung BB, Kleynhans A, Mittra R, Kim PY, Holien JK, Nagy Z, et al. A novel combination therapy targeting ubiquitin-specific protease 5 in MYCN-driven neuroblastoma. Oncogene. 2021;40(13):2367–81.
32. Xia Y, Ye B, Ding J, Yu Y, Alptekin A, Thangaraju M, et al. Metabolic Reprogramming by MYCN Confers Dependence on the Serine-Glycine-One-Carbon Biosynthetic Pathway. Cancer research. 2019;79(15):3837–50.
33. Bell E, Premkumar R, Carr J, Lu X, Lovat PE, Kees UR, et al. The Role of MYCN in the Failure of MYCN Amplified Neuroblastoma Cell Lines to G1 Arrest After DNA Damage. Cell Cycle. 2006;5(22):2639–47.
34. Burkhart CA, Cheng AJ, Madafiglio J, Kavallaris M, Mili M, Marshall GM, et al. Effects of MYCN antisense oligonucleotide administration on tumorigenesis in a murine model of neuroblastoma. Journal of the National Cancer Institute. 2003;95(18):1394–403.
35. Ryl T, Kuchen EE, Bell E, Shao C, Flórez AF, Mönke G, et al. Cell-Cycle Position of Single MYC-Driven Cancer Cells Dictates Their Susceptibility to a Chemotherapeutic Drug. Cell systems. 2017;5(3):237 – 50.e8.
36. Mossé YP, Fox E, Teachey DT, Reid JM, Safgren SL, Carol H, et al. A Phase II Study of Alisertib in Children with Recurrent/Refractory Solid Tumors or Leukemia: Children's Oncology Group Phase I and Pilot Consortium (ADVL0921). Clinical cancer research: an official journal of the American Association for Cancer Research. 2019;25(11):3229–38.
37. Mossé YP, Lipsitz E, Fox E, Teachey DT, Maris JM, Weigel B, et al. Pediatric phase I trial and pharmacokinetic study of MLN8237, an investigational oral selective small-molecule inhibitor of Aurora kinase A: a Children's Oncology Group Phase I Consortium study. Clinical cancer research: an official journal of the American Association for Cancer Research. 2012;18(21):6058–64.
38. Wang L, Chen C, Song Z, Wang H, Ye M, Wang D, et al. EZH2 depletion potentiates MYC degradation inhibiting neuroblastoma and small cell carcinoma tumor formation. Nature communications. 2022;13(1):12.
39. Chen L, Alexe G, Dharia NV, Ross L, Iniguez AB, Conway AS, et al. CRISPR-Cas9 screen reveals a MYCN-amplified neuroblastoma dependency on EZH2. The Journal of clinical investigation. 2018;128(1):446–62.

40. Ommer J, Selfe JL, Wachtel M, O'Brien EM, Laubscher D, Roemmele M, et al. Aurora A Kinase Inhibition Destabilizes PAX3-FOXO1 and MYCN and Synergizes with Navitoclax to Induce Rhabdomyosarcoma Cell Death. Cancer research. 2020;80(4):832–42.
41. Durbin AD, Zimmerman MW, Dharia NV, Abraham BJ, Iniguez AB, Weichert-Leahey N, et al. Selective gene dependencies in MYCN-amplified neuroblastoma include the core transcriptional regulatory circuitry. Nature genetics. 2018;50(9):1240–6.
42. Hogarty MD, Norris MD, Davis K, Liu X, Evageliou NF, Hayes CS, et al. ODC1 is a critical determinant of MYCN oncogenesis and a therapeutic target in neuroblastoma. Cancer research. 2008;68(23):9735–45.
43. Arlt B, Zasada C, Baum K, Wuenschel J, Mastrobuoni G, Lodrini M, et al. Inhibiting phosphoglycerate dehydrogenase counteracts chemotherapeutic efficacy against MYCN-amplified neuroblastoma. International journal of cancer. 2021;148(5):1219–32.
44. Morozova O, Vojvodic M, Grinshtein N, Hansford LM, Blakely KM, Maslova A, et al. System-level analysis of neuroblastoma tumor-initiating cells implicates AURKB as a novel drug target for neuroblastoma. Clinical cancer research: an official journal of the American Association for Cancer Research. 2010;16(18):4572–82.
45. Gustafson WC, Meyerowitz JG, Nekritz EA, Chen J, Benes C, Charron E, et al. Drugging MYCN through an allosteric transition in Aurora kinase A. Cancer cell. 2014;26(3):414–27.
46. Maris JM, Morton CL, Gorlick R, Kolb EA, Lock R, Carol H, et al. Initial testing of the aurora kinase A inhibitor MLN8237 by the Pediatric Preclinical Testing Program (PPTP). Pediatric blood & cancer. 2010;55(1):26–34.
47. Mollaoglu G, Guthrie MR, Böhm S, Brägelmann J, Can I, Ballieu PM, et al. MYC Drives Progression of Small Cell Lung Cancer to a Variant Neuroendocrine Subtype with Vulnerability to Aurora Kinase Inhibition. Cancer cell. 2017;31(2):270–85.
48. Dauch D, Rudalska R, Cossa G, Nault J-C, Kang T-W, Wuestefeld T, et al. A MYC–aurora kinase A protein complex represents an actionable drug target in p53-altered liver cancer. Nature medicine. 2016;22(7):744–53.
49. DuBois SG, Marachelian A, Fox E, Kudgus RA, Reid JM, Groshen S, et al. Phase I Study of the Aurora A Kinase Inhibitor Alisertib in Combination With Irinotecan and Temozolomide for Patients With Relapsed or Refractory Neuroblastoma: A NANT (New Approaches to Neuroblastoma Therapy) Trial. Journal of clinical oncology: official journal of the American Society of Clinical Oncology. 2016;34(12):1368–75.
50. DuBois SG, Mosse YP, Fox E, Kudgus RA, Reid JM, McGovern R, et al. Phase II Trial of Alisertib in Combination with Irinotecan and Temozolomide for Patients with Relapsed or Refractory Neuroblastoma. Clinical cancer research: an official journal of the American Association for Cancer Research. 2018;24(24):6142–9.
51. Zhou Y, Yan H, Zhou Q, Feng R, Wang P, Yang F, et al. Beta-Lapachone Attenuates BMSC-Mediated Neuroblastoma Malignant Transformation by Inhibiting Gal-3/Gal-3BP/IL6 Axis. Frontiers in

pharmacology. 2021;12:766909.

52. Zhou Y, Zhou Y, Wang K, Li T, Zhang M, Yang Y, et al. ROCK2 Confers Acquired Gemcitabine Resistance in Pancreatic Cancer Cells by Upregulating Transcription Factor ZEB1. Cancers. 2019;11(12).
53. Wang D, He J, Dong J, Wu S, Liu S, Zhu H, et al. UM-6 induces autophagy and apoptosis via the Hippo-YAP signaling pathway in cervical cancer. Cancer letters. 2021;519:2–19.

Figures

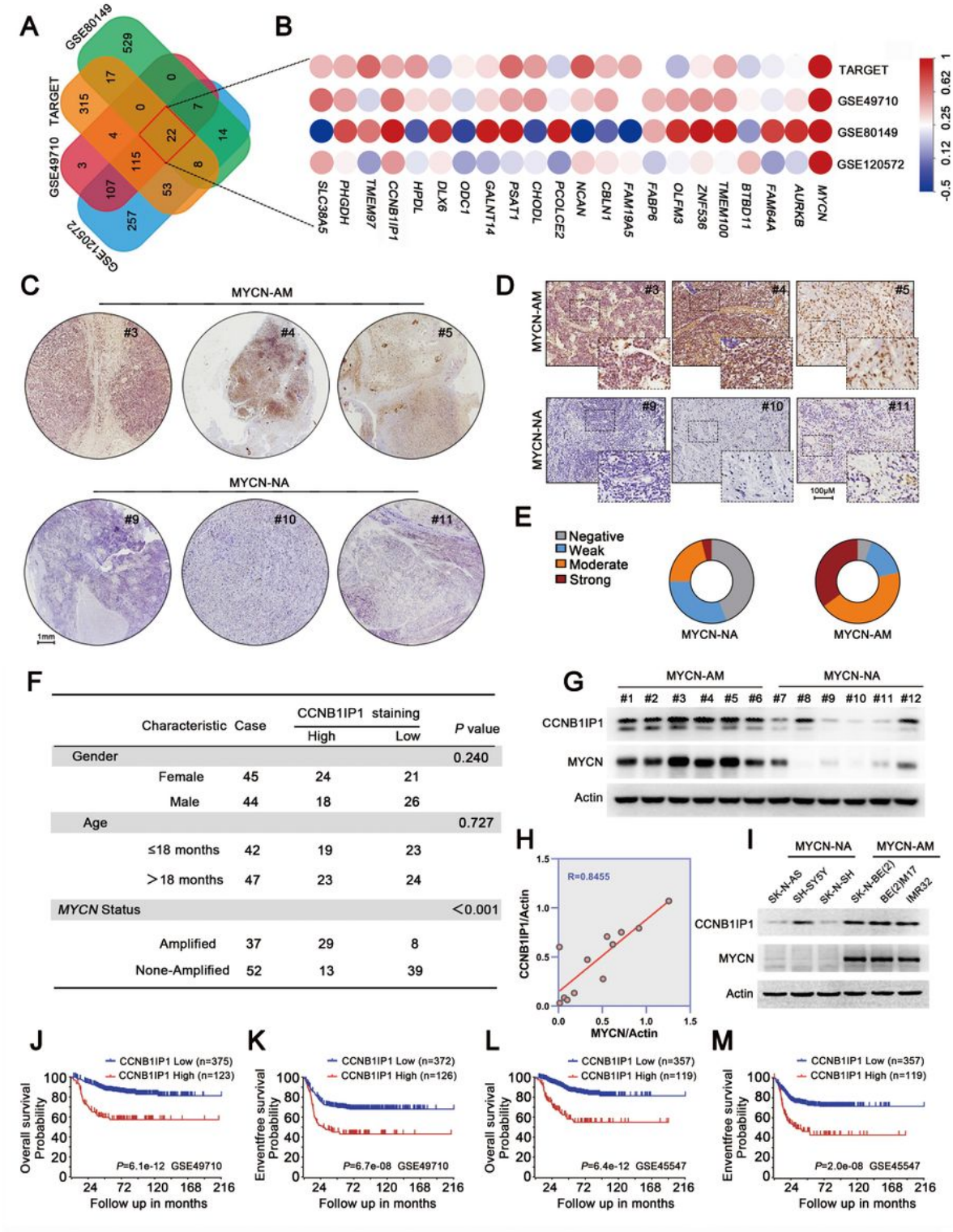

Figure 1

CCNB1IP1 overexpressed in MYCN-AM NB tissues and cell lines, and correlated with poor clinical characteristics. (A) Venn diagram reflecting shared upregulated differential genes between MYCN-AM and NA NB samples or cell lines from TARGET, GEO (GSE49710, GSE80149, GSE120572) datasets (log2FC > 1, $P < 0.01$). (B) Correlation between CCNB1IP1 and MYCN transcription levels from four different datasets. (C) IHC assay to detect CCNB1IP1 protein expression in MYCN-AM and NA NB sample tissues.

Scale bar = 1mm. (D) High magnification IHC images from **A**. Scale bar = 100μm. (E) IHC score of MYCN-AM and -NA NB. (F) Correlation of CCNB1IP1 expression with clinical characteristics of NB patients (age at diagnosis, gender and MYCN amplification status). The relative expression level of MYCN and CCNB1IP1 in MYCN-AM and NA NB specimens (G, H) and NB cells (I) was detected by IB assay. (H) Quantitative results of **G**. (J-M) Kaplan-Meier estimation of the OS and EFS based on the CCNB1IP1 transcriptome data from the TARGET and GSE45547 cohorts.

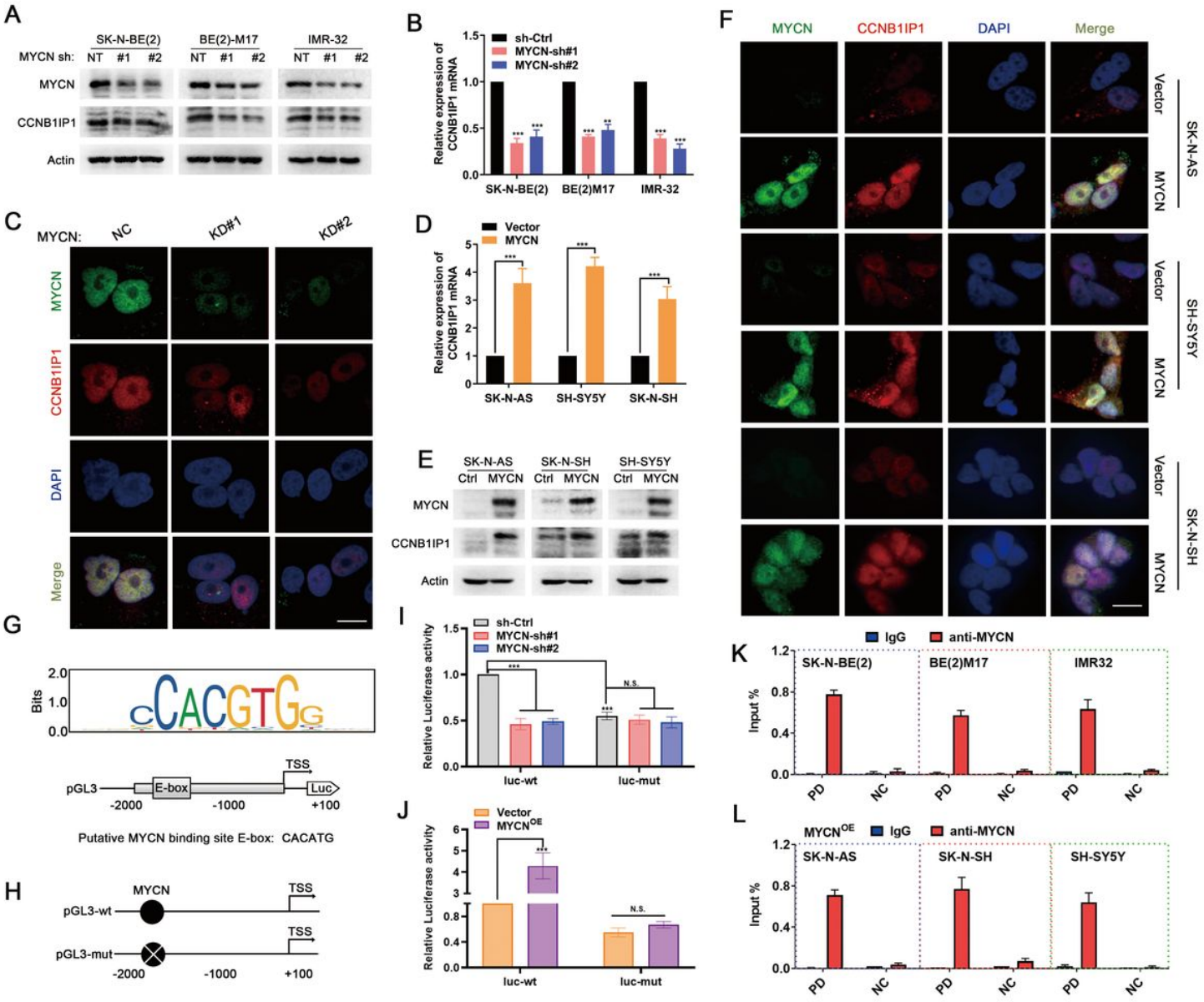

Figure 2

MYCN directly regulates expression and transactivation of CCNB1IP1 in NB cells. (A) Immunoblot (IB) assay of MYCN and CCNB1IP1 expression in SK-N-BE(2), BE(2)M17 and IMR32 cells was performed upon MYCN-shRNA knockdown for 48h. (B) Quantitative real-time PCR (qRT-PCR) was performed to detecte the mRNA expression of CCNB1IP1 in NB cells treated as **A**. (C) Representative IF images of IMR32 cell. MYCN, green; CCNB1IP1, red; DAPI, blue. Scale bar = 10μm. (D) qRT-PCR quantitation of CCNB1IP1 mRNA

expression in NB cells upon MYCN overexpressed. (E) IB assay of MYCN and CCNB1IP1 expression in SK-N-AS, SH-SY5Y and SK-N-SH cells treated as **D**. (F) Representative IF images. MYCN, green; CCNB1IP1, red; DAPI, blue. Scale bar = 10μm (G) Predicted MYCN binding site on the CCNB1IP1 promoter (2000bp upstream) using the jaspar database (https://jaspar.genereg.net/). (H) Schematic representation of the putative MYCN binding site E-box (-1973 to -1962 bp AATCACATGGCC) and the mutation site (-1973 to -1962 bp AATGTGATGGCC) on the CCNB1IP1 promoter. (I, J) Luciferase activity was assayed in MYCN-silenced or -overexpressed NB cells transfected with WT or mutant pGL3-CCNB1IP1 promoter constructs, and pRL-TK was used as an internal control. ChIP assay manifested MYCN enrichment in the promoter region of CCNB1IP1 in MYCN-AM NB cells (K) and MYCN-NA NB cells with MYCN expression (L). PD: Putative binding site; NC: Negative binding site. B, D, I-L, data represent the mean ± SD of at least three independent experiments (N.S., no significant differences; $^{**}P$<0.01 and $^{***}P$<0.001).

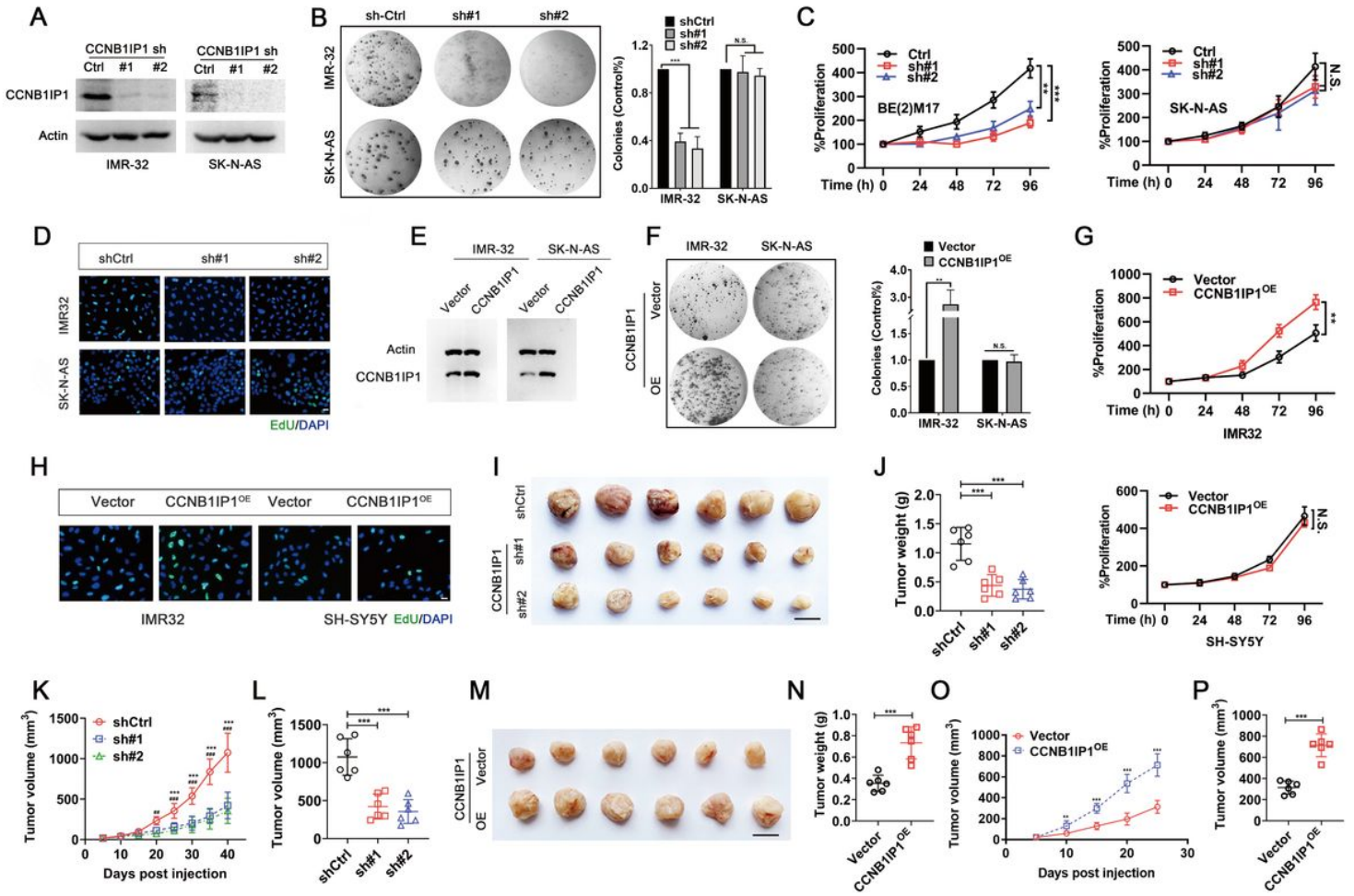

Figure 3

Altering the CCNB1IP1 expression selectively modulates the proliferation and growth of MYCN-AM NB cells. Two shRNAs targeting CCNB1IP1 with different sequences were transfected into NB cells (IMR32 and SK-N-AS cells) for 48h. (A) IB analysis of CCNB1IP1 protein levels was performed to detect the shRNA efficiency. (B) Colony-formation assay. (C) MTT assay. (D) EdU incorporation assay. Empty vector or vectors encoding CCNB1IP1 were transfected into NB cells for 48h. (E) IB analysis was performed to

detect the CCNB1IP1 protein expression level. (F) Colony-formation assay. (G) MTT assay. (H) EdU incorporation assay. (I) Image of subcutaneous tumor formation from IMR32 cells with or without CCNB1IP1 stably knockdown. Scale bar=10mm. (J) Tumor weight. (K) Volume changes of the subcutaneous tumor were measured periodically. (L) Tumor volume at the end of the study. (M) Image of CCNB1IP1 stably expressing IMR32 and vector-IMR32-derived subcutaneous tumors. Scale bar=10mm. (N) Tumor weight. (O) The volume changes of subcutaneous tumors were measured periodically. (P) Tumor volume at the study end point. B, C, F, G, J-L and N-P, Data represent the mean ± SD of at least three independent experiments (N.S., no significant differences; $^{*}P$<0.05; $^{**}P$<0.01 and $^{***}P$<0.001).

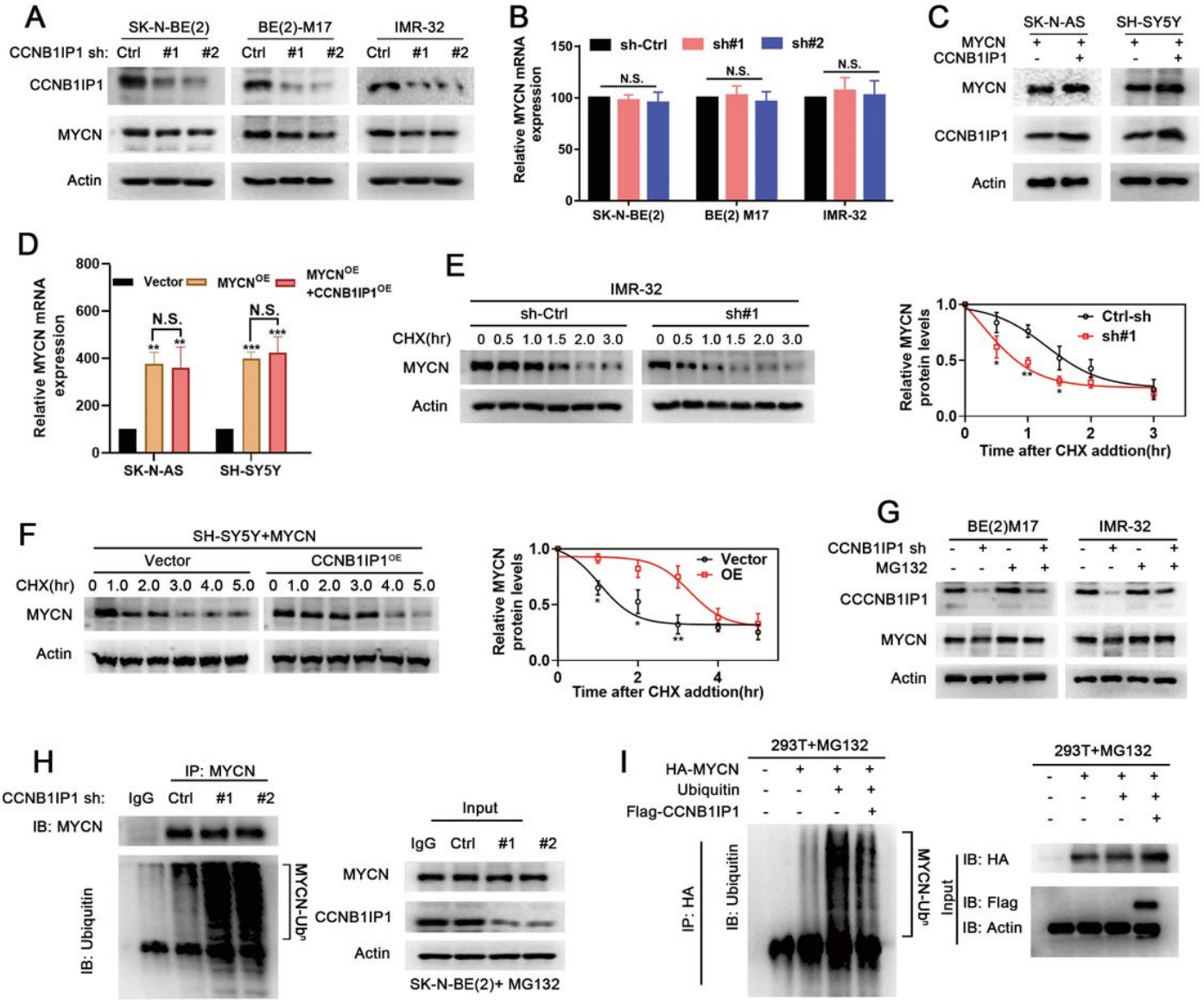

Figure 4

CCNB1I1P1 blocks MYCN protein ubiquitination and degradation. Two shRNAs targeting CCNB1IP1 were transfected into NB cells for 48h. (A) IB and (B) qRT-PCR analysis was performed to detected indicated protein and mRNA expression levels. Empty vector or plasmid encoding CCNB1IP1 were transfected into

MYCN-expressing non-amplified NB cells for 48h. (C) IB and (D) qRT-PCR analysis were performed to detected indicated protein and mRNA expression levels. (E, F) IB assay was performed for assessing the MYCN stability in NB cells with CCNB1IP1 knockdown or overexpressed were treated with CHX (10 μg/ml) for indicated time. (G) The protein expression of CCNB1IP1 and MYCN in CCNB1IP1-silenced or non-silenced NB cells stimulated with MG132 (20 μM) was detected by IB assay. (H) Co-IP assay was performed using anti-MYCN antibody in lysate of SK-N-BE(2) cell with or without CCNB1IP1 knockdown, and then anti-ubiquitin antibody was used for detecting MYCN ubiquitination level. (I) HA-MYCN, Ubiquitin and Flag-CCNB1IP1 plasmids were transfected alone or together into HEK-293T, and MYCN ubiquitination level was detected by co-IP assay. B, D, E and F, data represent the mean ± SD of at least three independent experiments (N.S., no significant differences; $^{*}P$ 0.05; $^{**}P$ 0.01 and $^{***}P$ 0.001).

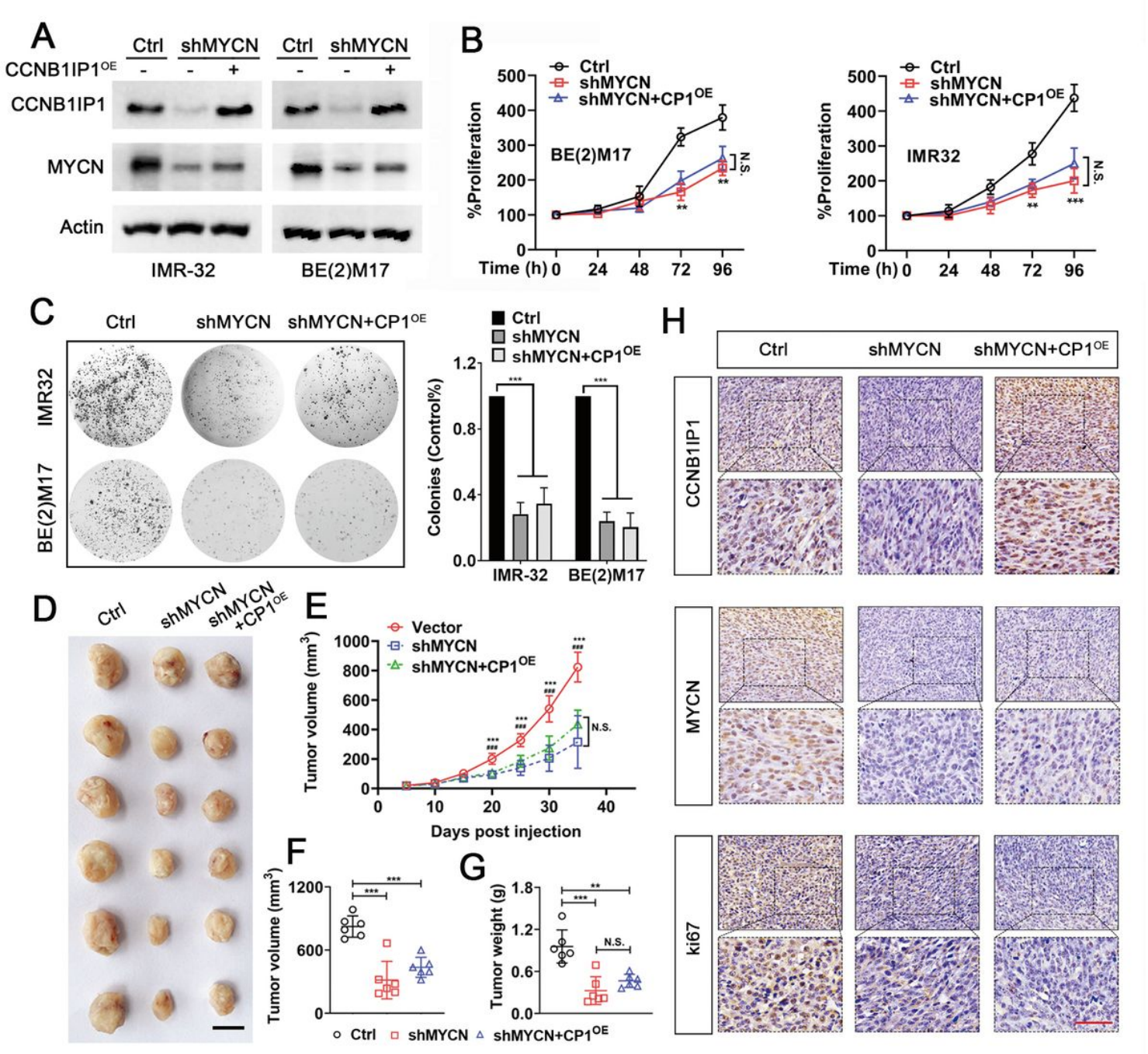

Figure 5

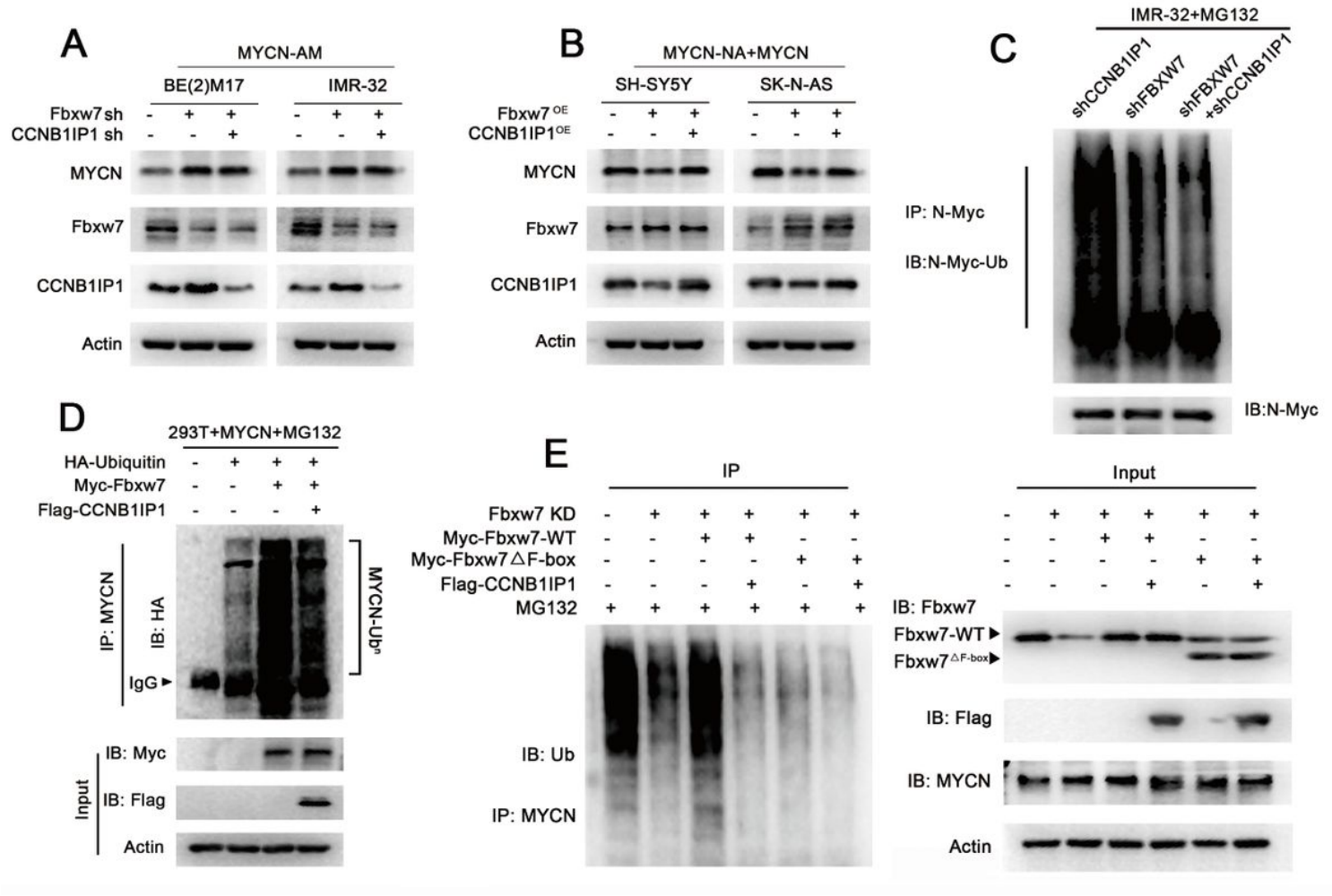

Figure 6

CCNB1IP1 stabilizes MYCN protein by disrupting Fbxw7-mediated ubiquitination. IB analysis of MYCN, Fbxw7 and CCNB1IP1 protein expression. (A) BE(2)M17 and IMR32 cells infected with shFbxw7 alone or together with shCCNB1IP1. (B) SH-SY5Y and SK-N-AS cells overexpressed Fbxw7 alone or together with

CCNB1IP1. (C) In vivo ubiquitination assay of MYCN in IMR32 cell with knockdown of Fbxw7 and CCNB1IP1 alone or together (D) or MYCN-expressing HEK293T cell infected with plasmids encoding HA-Ubiquitin, Myc-Fbxw7 and Flag-CCNB1IP1 alone or together (E) or IMR32 cell knockdown of Fbxw7 infected with plasmids encoding Myc-Fbxw7-WT, Myc-Fbxw7$^{\triangle F\text{-box}}$ and Flag-CCNB1IP1 alone or together.

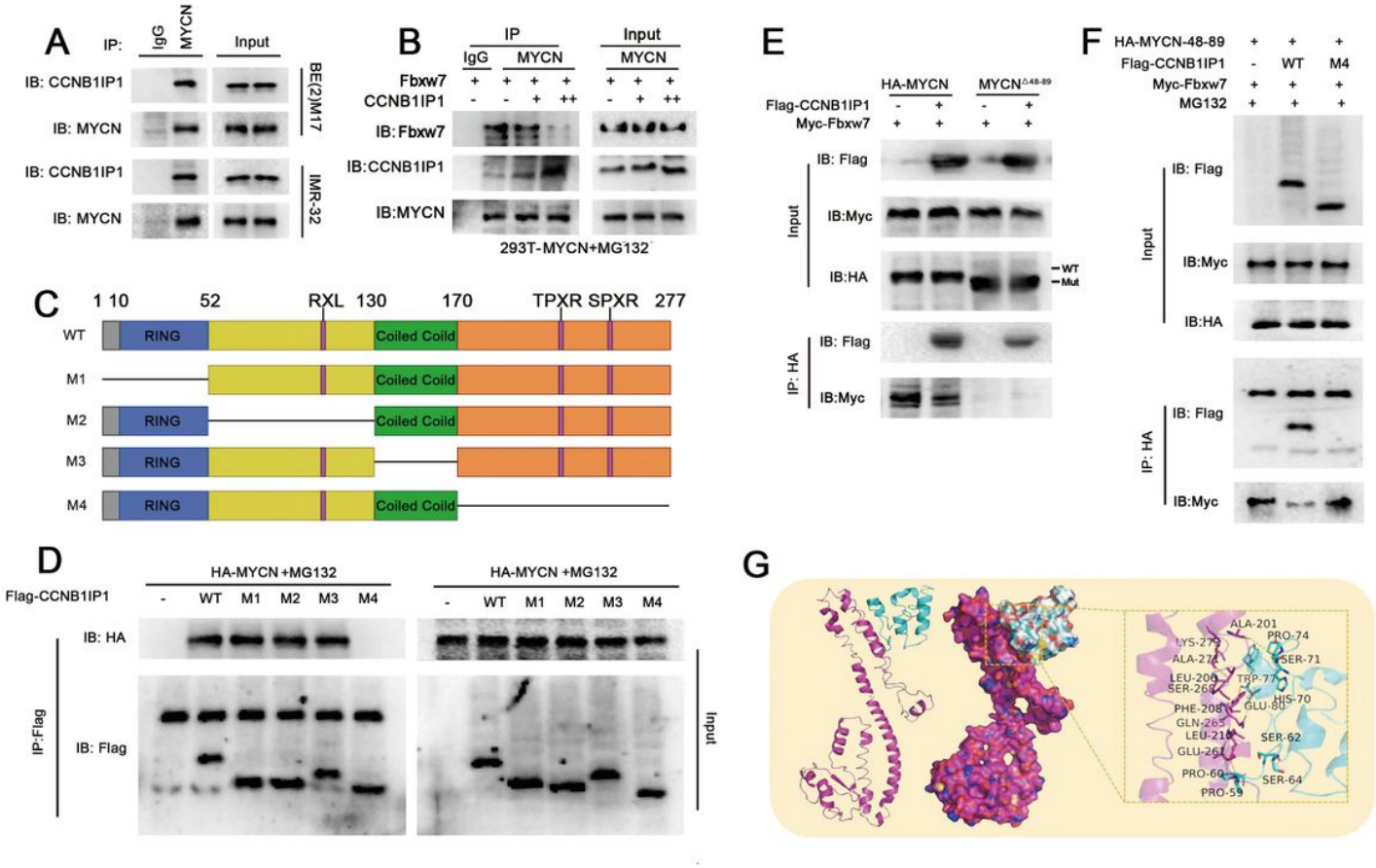

Figure 7

CCNB1IP1 stabilizes MYCN protein by competing with Fbxw7 for MYCN binding. (A) Endogenous interaction between CCNB1IP1 and MYCN. Co-IP assay was performed using anti-MYCN antibody and IgG was used as a negative control. (B) Interference of exogenously expressed CCNB1IP1 with the Fbxw7-MYCN interaction was detected by co-IP assay. (C) Schematic depiction of CCNB1IP1 WT and truncated mutants. (D) The interaction between MYCN and CCNB1IP1 WT or truncated mutants was determined in HEK293T cell transfected separately with Flag-CCNB1IP1 WT and different truncated mutants along with HA-MYCN. Co-IP assay to analyze the competitive binding of CCNB1IP1 to MYCN with Fbxw7. (E) HEK293T cell expressing HA-tagged MYCN WT or MYCN$^{\triangle 48\text{-}89}$ mutant was transfected with plasmids encoding Myc-Fbxw7 alone or together with Flag-CCNB1IP1. (F) HEK293T cell expressing Myc-Fbxw7 was transfected with plasmids encoding HA-MYCN WT or MYCN$^{48\text{-}89}$ mutant alone or together with Flag-CCNB1IP1. (G) The binding mode of the complex CCNB1IP1 with MYCN (AA 59 to 138). The backbone of protein was rendered in tube and colored. CCNB1IP1 (down) and MYCN (up) protein is rendered by the surface. The detail binding mode of CCNB1IP1 with MYCN (right). Yellow dash represents hydrogen bond or salt bridge.

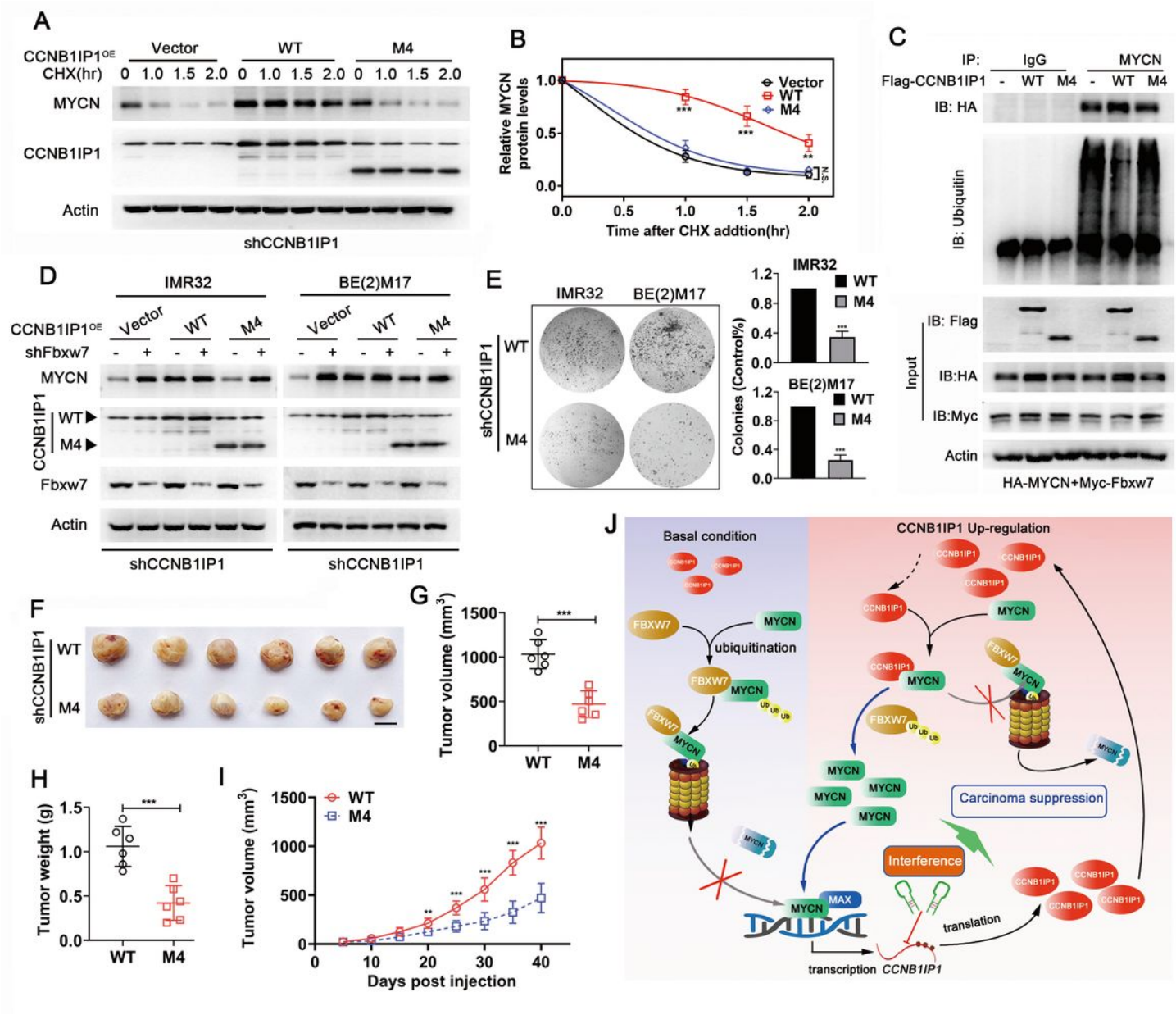

Figure 8

The C-terminal domain of CCNB1IP1 is essential for MYCN stabilization, and promotion of tumor growth. (A) Protein half-life analysis of MYCN in shCCNB1IP1-IMR32 cell with re-expression of CCNB1IP1 WT or M4 mutant plasmids. Empty vector was used as a negative control. Cells were treated with CHX (10 μg/ml) and lysates were harvested for IB analysis. (B) Quantification of **A**. (C) Ubiquitination of MYCN was detected in HEK293T cell transfected with HA-MYCN alone or together with Myc-Fbxw7, Flag-CCNB1IP1 WT or M4 mutant. (D) CCNB1IP1 WT or M4 mutant was re-expressed alone or co-transfected with Fbxw7-shRNA in CCNB1IP1-depleted NB cells. IB assay was performed to detect the expression of specific protein. (E) Colony formation assays were performed in with shCCNB1IP1-IMR32 and -BE(2) M17 cells transfected with CCNB1IP1 WT or M4 mutant plasmids. B and E, data represent the mean ± SD of at least three independent experiments (N.S., no significant differences; $^{**}P$ 0.01 and $^{***}P$ 0.001). CCNB1IP1-depleted IMR32 cell stably re-expressing CCNB1IP1 WT or M4 mutant were then subcutaneously

inoculated into nude mice to construct xenograft tumor models. (F) Images of the xenografts. Scale bar=10mm. (G) Volume changes of subcutaneous tumors were measured periodically. (H) Tumor volume (I) and weight at the end point. (J) Proposed model of the disruption of Fbxw7-mediated MYCN ubiquitination degradation by CCNB1IP1 in NB cells. G-I, data represent mean ± SD, ($^{**}P < 0.01$ and $^{***}P < 0.001$).

Supplementary Files

This is a list of supplementary files associated with this preprint. Click to download.

- Supplementaryfiles.pdf